ISH Journal of Hydraulic Engineering

ISSN: 0971-5010 (Print) 2164-3040 (Online) Journal homepage: https://www.tandfonline.com/loi/tish20

Seepage through earth dam with clay core and toe drain: the Casagrande–Numerov analytical legacy revisited

A.R. Kacimov, A. Al-Maktoumi & Yu.V. Obnosov

To cite this article: A.R. Kacimov, A. Al-Maktoumi & Yu.V. Obnosov (2019): Seepage through earth dam with clay core and toe drain: the Casagrande–Numerov analytical legacy revisited, ISH Journal of Hydraulic Engineering, DOI: 10.1080/09715010.2019.1633694

To link to this article: https://doi.org/10.1080/09715010.2019.1633694

ISH JOURNAL OF HYDRAULIC ENGINEERING
https://doi.org/10.1080/09715010.2019.1633694

Taylor & Francis
Taylor & Francis Group

Seepage through earth dam with clay core and toe drain: the Casagrande–Numerov analytical legacy revisited

A.R. Kacimov[a], A. Al-Maktoumi[a] and Yu.V. Obnosov[b]

[a]Department of Soils, Water and Agricultural Engineering, Sultan Qaboos University, Muscat, Sultanate of Oman; [b]Institute of Mathematics and Mechanics, Kazan Federal University, Kazan, Russia

ABSTRACT

Seepage through a zoned earth-filled dam with a vertical clay core, two permeable shoulders and toe drain are studied. Seepage through the core and the downstream shoulder are coupled. The flow rate and phreatic surface are found. The hodograph method is used, viz. a conformal mapping of a rectangle in the complex potential plane onto a circular triangle. Numerically, MODFLOW 2005 simulated seepage with the refraction of the streamlines at the interfaces between the core and both shoulders.

ARTICLE HISTORY
Received 23 January 2019
Accepted 16 June 2019

KEYWORDS
Complex potential-hodograph method; phreatic surface–refraction; MODFLOW numerical simulations

1. Introduction

Hundreds of earth-filled dams have been constructed in the MENA region (see e.g. Al-Saqri et al. 2016, Jaafar 2014) for interception of wadi runoff, flood protection and managed aquifer recharge of groundwater through the beds of dams' reservoirs. These hydraulic structures (Figure 1(a)) are often designed to withstand a relatively low head, H_0, of several meters of reservoir water, retained after rare flashfloods. The embankments are long, up to several kilometers in length, L_c, along the crest (Al-Saqri et al. 2016; Kacimov and Brown 2015) and demarcate the reservoir area which most of the time is dry. Consequently, unlike dams designed for hydropower generation requiring high H_0 and low L_c (gorge sites), the recharge dams in flat areas are designed and constructed with a tradeoff between the value of land allocated for the structure (mainly reservoir), rapidity of infiltration and groundwater replenishment, safety of the embankment and cost of construction. The embankment shoulders are made by bulldozing a cheap local soil (alluvium of a wadi flood plain), which is highly permeable. A low-permeable clay core reduces seepage. The core is the most expensive component of the embankment and therefore it is made as thin as possible. The tailwater is most often empty such that these dams are often called 'dry' (Sumi 2008). In rare cases, the tailwater is fed by spillway flow over the dam crest and short periods of releasing water from the reservoir through sluice gates. Boiling, heaving, backward erosion, piping, sloughing, suffusion and other seepage-triggered phenomena can destabilize the embankments (see e.g. Design 1987). In order to forestall exit seepage gradients a toe drain (a horizontal filter in Figure 1(a)) is constructed in the downstream shoulder. This drain is made of a course material (graded gravel). It prevents outcropping of a phreatic surface on the downstream soil slope. The drain diverts the seeped water to a stilling basin or directly to the recharge zone downstream of the dam.

A Darcian seepage in cored and drained dams has been theoretically studied since Kozeny, Terzaghi, Casagrande and Pavlovsky (see e.g. Polubaronova-Kochina, 1962, hereafter abbreviated as PK). Nowadays, the textbooks and engineering design charts reflect these 'old' analytical formulae (see e.g. Cedergren 1989; Design 1987; FEMA 2011; ICOLD 2013; Istomina 1957; National Research Council 2012; Nichiporovich 1973; Peter 1982; Tanchev 2014; The International Levee (2013), Wolff (2002), Zhang et al. (2016), Zhilenkov 1968).

Most recent studies of seepage through earth dams use numerical models (FEM, BEM, FDM and CFD) that allows to take into account steady-state and transient flows through porous composites making the shoulders-core-filter in Figure 1(a) (zoned dams and anisotropic soil fillings) for purely saturated and saturated-unsaturated flows (see e.g. Bardet and Tobita 2002; Borja and Kishnani 1991; Darbandi et al. 2007; Liggett and Liu 1979; Ouria and Toufigh 2009; Tayfur et al. 2005) that was not possible in analytical models. Unfortunately, the 'dam problem', analytically solved by PK for 2-D steady seepage through a rectangular homogeneous embankment without capillarity, is now days seldom used (see e.g. Fukuchi 2018) as a benchmark for testing numerical models, which are compared with each other rather than with analytical formulae. In applied mathematics, this analytical solution by PK formed a whole branch of 'free-moving boundary value problems' (see e.g. Caffarelli and Friedman 1978; Friedman et al. 1987; Martin and Vázquez 2013; Strack 2017), with numerous ramifications in other fields of mathematical physics (Crank 1984).

One of the objectives of this paper is to revisit the old analytical methods and solutions. We obtain new analytical formulae for comparisons with simulations by FDM (MODFLOW). This comparison of new and old analytical results with numerical ones is a routine because of the following:

CONTACT A.R. Kacimov anvar@squ.edu.om

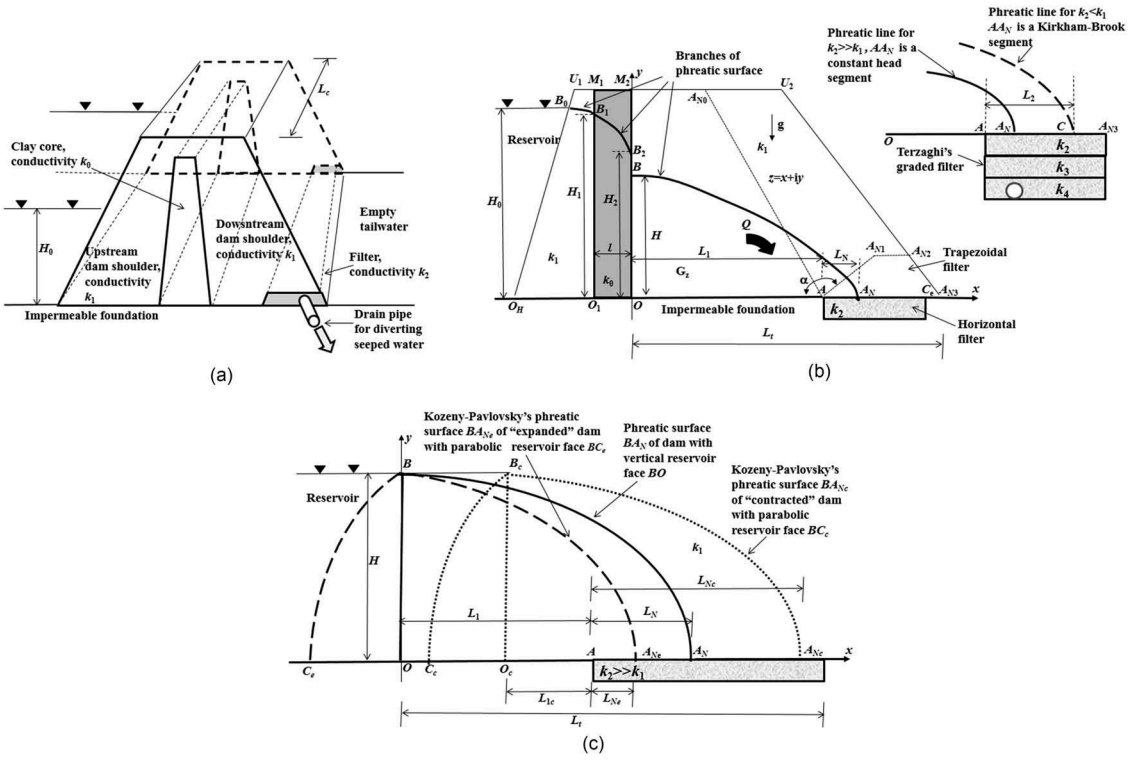

Figure 1. (a) 3-D earth dam with a core. (b) Vertical cross-section of flow domain for seepage through an earth-filled dam. (c) Vertical-face embankment and its free surface with seepage into an unclogged toe drain (solid curves) sandwiched between Kozeny-Pavlovsky's 'expanded' parabolic-face dam (dashed curves) and 'contracted' dam (dotted curves).

- all numerical codes use analytical solutions as benchmarks,
- commercial numerical packages are often not available when preliminary back-of-an envelope calculations are carried out by engineers at the stage of dam design,
- most numerical packages are parameter-demanding and it is recommended to apply a step-wise approach, starting from the bottom of scaffolding complexity of models where analytical solutions are indispensable,
- numerical packages operate always with dimensional input parameters while analytical solutions can be graphed and tabulated in dimensionless formats that makes the analysis of trends easier,

among others.

Figure 1(b) below (see also Design 1987; The International Levee 2013) shows a vertical cross-section of a dam placed on an impermeable horizontal foundation Ox. The vertical axis Oy of a Cartesian coordinate system coincides with an interface between the core and upstream shoulder. In Figure 1(b) the core is rectangular and made of clay of hydraulic conductivity k_0. Two dam shoulders have hydraulic conductivity k_1. In a newly constructed dam, the material of the toe drain is highly permeable, of a conductivity k_2 and a double inequality $k_2 \gg k_1 \gg k_0$ holds. A free (phreatic) surface in Figure 1(b) has three branches: B_0B_1 in the upstream shoulder, B_1B_2 in the core and BA_N in the downstream shoulder. The segment BB_2 is often modeled as a seepage face (or 'internal seepage face' in the terminology of Wu et al. 2013). A horizontal toe drain AC_e, located distance L_1 from the downstream face of the core, intercepts the seepage discharge Q. The magnitude of Q should be small, and the locus of BA_N should be low that is achieved by selecting various counter-seepage designs (see e.g. Rice and Duncan 2010).

The dashed line AA_{N0} in Figure 1(b) shows a tailwater slope of a dam without any drain and the trapezium AA_{N1} A_{N2} $A_{N3}A$ depicts a tailwater filter which can be placed inside the embankment or on the slope as a load (see e.g. Moran and Toledo 2011). The angle α between the impermeable foundation and AA_{N1} in Figure 1(b) varies from 0 to π. The latter value corresponds to the case of the toe drain in Figure 1(a).

Below a steady-state seepage is considered, i.e. a basic regime from which the design of dams starts (see e.g. Casagrande 1937; Fukuchi 2018; Kamble et al. 2014). The motivation is two-fold. First, the theory of holomorphic functions (PK, Strack 2017) is applied for obtaining new analytical solutions to problems of free-boundary, steady 2-D seepage through a cored dam shown in Figure 1(b). This theory deals with characteristic flow functions presented in planes of complex variables that is possible if the hydraulic head in seepage obeys Laplace's equation. Modern computer algebra, *viz.* Wolfram's *Mathematica* (1991) makes the obtained analytical solutions user/engineer-friendly. Second, a standard FDM package (MODFLOW) is utilized for comparisons of numerical and analytical models.

2. Seepage through cored dam to unclogged toe drain

The key flow characteristics of 2-D, steady, capillarity-free flow (Q, L_N and the shape of BA_N in Figure 1(b) where the width of the downstream shoulder is L_t) are evaluated and compared with approximate 1-D formulae (the Dupuit-Forchheimer, DF, approximation), used by engineers since Shaffernak–Casagrande (see e.g, Chahar 2004; Fukuchi

2018; Junghanns and Oestreich 1989; Mishra and Singh 2005).

2.1. Seepage through a downstream shoulder

The inequality $k_1 \gg k_0$ holds in this subsection and hence we ignore the hydraulic resistance of the upstream shoulder and assume that the hydraulic head there is constant, i.e. $H_0 = H_1$. Consequently, the upstream vertical face of the core, B_1O_1, is a constant-head boundary, and the branch B_0B_1 of the free surface in the upstream shoulder is a horizontal segment. The validity of this assumption will be later checked by MODFLOW.

Numerov (see Aravin and Numerov, 1953 and PK) studied flow in the downstream shoulder of Figure 1(b), with a trapezoidal filter of an arbitrary angle α. The segment AA_{N1} in Figure1 (b) was a constant-head boundary, i.e. a seepage face segment along AA_{N1} was ignored. Numerov used a conformal mapping of a rectangle in the complex potential domain onto an auxiliary domain. Then, in this domain, he solved the so-called Hilbert problem (see e.g. Gakhov 1966) for the complex physical coordinate. Numerov's solution is prohibitively complicated and – to the best of our knowledge – is not used in the engineering practice. An alternative hodograph method (see e.g. Obnosov et al. 2015) is used below for a special case of $\alpha = \pi$ in Figure 1(b), for which the drain segment is both a constant head and constant pressure boundary. Obviously, for this horizontal outlet boundary the Shaffernak or Casagrande engineering formulae (limited to the range $0 < \alpha < \pi/2$) are not applicable.

Cartesian coordinates xOy (Figure 1(b)) and a complex physical coordinate $z = x+iy$ are introduced. The hydraulic head $h(x,y)$ in G_z is a harmonic function. A complex potential $w = \varphi + i\psi$ is introduced, where $\phi = -k_1 h$ is the velocity potential, and $\psi$is a stream function. The Darcian velocity, $\vec{V}(x,y)$, obeys the relation $\vec{V}(x,y) = -k_1 \nabla h$. A complex Darcian velocity is $V = u+iv$, where $u(x,y)$ and $v(x,y)$ are the horizontal and vertical components of $\vec{V}$.

First, as in PK, the hydraulic head along BO is assumed to be – H, where $H > 0$ is given. The flow rate Q_N is a part of solution. A horizontal bed OA of a given length L_1 is a streamline $\psi = 0$. Along the free-surface BA_N two boundary conditions are satisfied: $\psi = Q_N$ and $\phi + k_1 y = 0$ Along the segment AA_N, $\phi = 0$ Consequently, the complex potential domain G_w is a rectangle depicted in Figure 2(a).

The rectangle G_w is mapped onto an auxiliary half plane G_ζ (Figure 2(b)) by the Schwarz–Christoffel integral:

$$w(\varsigma) = c_1 \int_{-a}^{\varsigma} \frac{\mathrm{d}t}{\sqrt{(a^2 - t^2)(t^2 - 1)}} + \mathrm{i}Q_N, \tag{1}$$

where a is the affix of point A in G_ζ to be found later. The mapping constant c_1 is determined from the equality $w_B = -k_1 H + \mathrm{i}Q_N$ as:

$$c_1 = -\frac{k_1 H}{I_1}, \; I_1 = \int_{-a}^{-1} \frac{\mathrm{d}t}{\sqrt{(a^2 - t^2)(t^2 - 1)}}. \tag{2}$$

For the sake of brevity, here and below the expressions of I_1 and similar integrals via elliptic functions are omitted.

By considering the straight lines BA and A_NA are chords of circles of infinite radius, the hodograph domain G_V is regarded as a circular triangle (Figure 2(c)) which is inversed to a half-strip G_U of the function $\mathrm{d}z/\mathrm{d}w$ (Figure 2 (d)). G_U is mapped onto G_ζ by the Schwarz-Christoffel formula as:

$$\begin{aligned} \frac{\mathrm{d}z}{\mathrm{d}w}(\varsigma) &= d_1 \int_{\varsigma}^{a} \frac{\mathrm{d}t}{\sqrt{a^2 - t^2}(t+1)} \\ &= \frac{d_1}{\sqrt{a^2 - 1}} \log\left[\frac{\varsigma + a^2 + \sqrt{a^2 - 1}\sqrt{a^2 - \varsigma^2}}{a(\varsigma + 1)}\right] \end{aligned}, \tag{3}$$

where the mapping constant d_1 is found from the condition $\mathrm{d}z/\mathrm{d}w(-a) = -\mathrm{i}/k_1$ (see Figure 2(c)) as:

$$d_1 = -\sqrt{a^2 - 1}/(\pi k_1). \tag{4}$$

The integration appearing in Equation (3) is carried out by substituting $1 + t = X^*$, $\mathrm{d}t = \mathrm{d}X^*$, which converts the integral into a standard form to use a mathematical table (Gradshteyn and Ryzhik, 1962). The integration constant has been determined by applying the condition at vertex A and implemented in Equation (3).

with differentiation of Equation (1) involved, as:

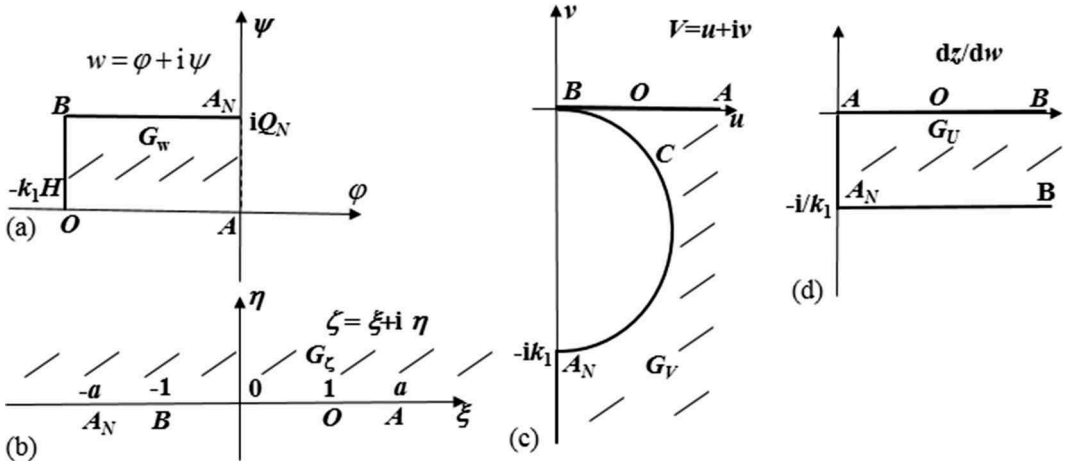

Figure 2. Domains of characteristic functions for Numerov's problem with a horizontal equipotential drain (shown earlier in Figure1b): complex potential domain (a), auxiliary plane (b), hodograph domain (c), inverted hodograph (d).

$$z(\varsigma) = \int_1^{\varsigma} \frac{\mathrm{d}z}{\mathrm{d}\varsigma}\mathrm{d}\varsigma = \frac{H}{\pi I_1}\int_1^{\varsigma} \log\left[\frac{\varsigma + a^2 + \sqrt{a^2-1}\sqrt{a^2-\varsigma^2}}{a(\varsigma+1)}\right] \frac{\mathrm{d}\varsigma}{\sqrt{a^2-\varsigma^2}\sqrt{\varsigma^2-1}} \tag{5}$$

Here $\mathrm{d}z/\mathrm{d}w$and $\mathrm{d}w/\mathrm{d}\varsigma$ are found from Equations (3) and (1).

From Equation (5), at point *A* in Figure 1(b)

$$L_1{}^* = \frac{L_1}{H} = \frac{1}{\pi I_1}\int_1^{a} \log\left[\frac{\varsigma + a^2 + \sqrt{a^2-1}\sqrt{a^2-\varsigma^2}}{a(\varsigma+1)}\right] \frac{\mathrm{d}\varsigma}{\sqrt{a^2-\varsigma^2}\sqrt{\varsigma^2-1}}. \tag{6}$$

The parameter *a* is evaluated from Equation (6) using the **FindRoot** routine of *Mathematica*, with integrals computed by the **NIntegrate** routine. Any other commercial (e.g. MATLAB, COMSOL), or public (e.g. Python) code can be equivalently used. It is noteworthy that the determination of *H* in the composite section of Figure 1(b) has been dealt separately.

Then, from Equations (1–2) at point *B* (ζ = 1):

$$Q_N^* = \frac{Q_N}{k_1 H} = \frac{I_0}{I_1},\ I_0 = \int_{-1}^{1} \frac{\mathrm{d}t}{\sqrt{(a^2-t^2)(1-t^2)}}, \tag{7}$$

wherefrom the dimensionless flow rate is evaluated.

Figure 3(a) shows $Q_N^*(L_1^*)$ calculated from Equations (6) and (7) (curve 1). A dimensionless Numerov's approximation, Q_{ap}^* (see PK, p. 223 and Kacimov and Obnosov 2012) is:

$$Q_{ap}^* = \frac{Q_{ap}}{k_1 H},\ Q_{ap} = k_1 \frac{H^2}{L_1 + \sqrt{{L_1}^2 + 1/3H^2}} \tag{8}$$

Equation (8) is plotted in Figure 3(a) as curve 2.

Another approximate formulae follow from the Kozeny-Pavlovsky (hereafter abbreviated as KP) solution of a 2D phreatic flow from an 'upstream infinity' towards a slot drain (see PK, Chapter II, Section 10). The analysis below follows Mishra and Parida (2006). In the KP problem shown in Figure 1(c), the phreatic surface is half of a parabola BN_e (dashed line). The flow net is made of two families of mutually orthogonal confocal half-parabolas (streamlines and constant-head lines). Then, the vertical upstream face *BO* of a homogeneous embankment (held at a reservoir level *H)* can be sandwiched between two parabolic upstream faces of fictitious embankments subject to the same head drop *H*. The first one has an upstream face BC_e (Figure 1(c)), which is obtained by 'expansion' of the segment *BO* (solid line in Figure 1(c)) of the real embankment. The corresponding flow rate is Q_e and a fictitious phreatic surface, BA_{Ne}, is a segment of parabola which outcrops at the horizontal filter such that a segment AA_{Ne} has a length L_{Ne}. The second KP domain is made by contraction of the real *BO* in Figure 1(c) to

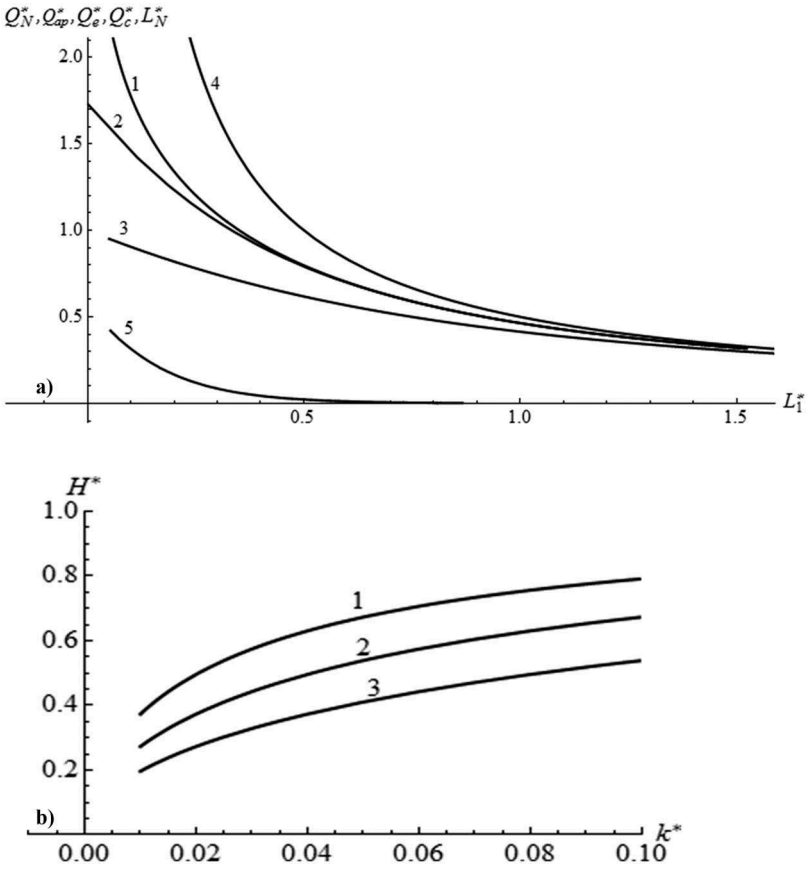

Figure 3. (a) Dimensionless flow rates through the downstream shoulder in Figure1b, non-conjugated with the flow through the core, rigorous Q_N^* for potential 2-D model (curve 1), approximation Q_{ap}^* by eqn. (8), KP approximations Q_e^* (curve 3), Q_c* (curve 4) and dimensionless length L_N^* of an unclogged drain (curve 5), all as functions of distance L_1^* between the core and shoulder. (b) Dimensionless height *H** of the 'internal seepage face' for a coupled flow through the core and downstream shoulder as a function of relative conductivity *k** of the core for dimensionless widths of the core *l** = 1/4,1/8 and 1/16 (curves 1–3, correspondingly).

a fictitious parabolic-face B_cC_c (a dotted contour in Figure 1(c)), which corresponds to a vertical-face embankment B_cO_c located distance L_{1c} from point A in Figure 1(c). The corresponding flow rate is Q_c and phreatic surface is B_cA_{Nc}. According to Mishra and Parida (2006), the KP solution reads:

$$Q_e^* = \frac{Q_e}{k_1 H} = \frac{1}{L^*{}_1 + \sqrt{L^*{}_1{}^2 + 1}},\ L^*{}_{Ne} = 0.5Q_e^*,$$
$$Q_c^* = \frac{Q_c}{k_1 H} = \frac{1}{2L^*{}_1},\ L^*{}_{Nc} = 0.5Q_c^*. \quad (9)$$

PK emphasized that Equation (9) gives exactly the same values of the flow rate as the DF approximation in a dam problem where a face of the tailwater is assumed to be a vertical constant-head segment (a seepage face boundary is ignored in the DF model).

USBR (*Design*, 1987) stipulates the minimum length of L_N as one of the main criteria in dam design. For calculation of L_N Equation (5) is modified as:

$$\frac{dz}{dw} = \frac{i}{k_1}\arctan\frac{\sqrt{a^2-1}\sqrt{\varsigma^2-a^2}}{\varsigma + a^2},$$
$$\frac{dw}{d\varsigma} = \frac{ik_1 H}{I_1\sqrt{\varsigma^2-a^2}\sqrt{\varsigma^2-1}} \quad (10)$$

and integrated from a to ∞ and from $-\infty$ *to* $-a$. Curve 5 in Figure 3(a) shows the dimensionless length $L_N^* = L_N/H$ of the 'active' segment of the horizontal drain.

From the comparison theorems (see e.g. Gol'dshteĭn and Entov 1994; Ilyinsky and Kacimov 1992; Ilyinsky et al. 1998) two double inequalities follow:.

$$Q_e^* < Q_N^* < Q_c^*,\ L_{Ne}^* < L_N^* < L_{Nc}^*$$

They give an upper and lower bound for Q_N^* and L_N^* of a real embankment.

From comparison of curve 1 with curves 2–4 in Figure 3(a), one can see that at $L_1^* < 1$ (relatively 'narrow' shoulders) the approximations give significantly over-, under-estimated values of the flow rate than the exact formulae. Curve 5 in Figure 3(a) illustrates that for 'narrow' shoulders, the size of AA_N in Figure 1(b) is relatively large. In the vicinity of the outlet segment AA_N, most deleterious suffusion and drain-clogging phenomena evolve in 'old' embankments.

2.2. Coupled flow through core and downstream shoulder

Now, the flows in the core and downstream shoulder of Figure 1(b) are coupled. In this case, H is a part of solution, while $H_1 = H_0$ is given. For the case of $\alpha = \pi/2$ (vertical segment AA_{N0} in Figure 1(b)), Kacimov and Obnosov (2012) illustrated how a potential 2-D flow in the core can be conjugated with a DF flow in the downstream shoulder. As Figure 3 shows, the DF approximation is poor for small L_1 in Figure 1(b).

A full 2-D solution for flow in the core alone, without conjugation with flow in the downstream shoulder (Figure 1(b)), is given by PK (see Kacimov and Obnosov 2016). In the PK problem, H_1 and H are given, but the locus of point B_2 (or H_2 in Figure 1(b)) is not. Hydraulic head, $h_0(x,y)$, and stream function $\psi_0(x,y)$, are introduced in the core where both functions obey the Laplace equation. In notations of Figure 1(b), the flow domain is bounded by a vertical face B_1O_1 where $h_0(-l,y) = H_1$, a vertical face OB where $h_0(0,y) = H < H_1$, a no-flow segment O_1O where $\psi_0(x,0) = 0$, a free-surface B_1B_2 where $\psi_0 = Q_{Nc}$ (where Q_{Nc} is the flow rate through the core), $h_0(x,y)$-y = 0 and a seepage face B_2B where $h_0(0,y)$-y = 0. For flow in Figure 1(b), this boundary value problem (BVP) is an approximation, valid for $k_1 \gg k_0$. The approximation ignores flow refraction in the core and downstream. We recall (PK, Strack 2017) that in seepage flows refraction on a heterogeneity of two porous media means that a streamline at the interface of these media is continuous but not smooth that is mathematically equivalent to the conditions of continuity of a normal component of the Darcian velocity and a jump of the tangential component. Figure 4 shows two refracting internal streamlines. As analyzed by Liggett and Liu (1979), a refracted phreatic surface B_0B_r approaches the interface Oy tangentially to it, similarly with Casagrande's three cases illustrated in Liggett and Liu (their Figure 3(b,c,d)), which all degenerate into what is shown in our Figure 4. In the limit $k_1 \to \infty$, the refraction problem transforms to the PK problem with a seepage face. In this problem (see the corresponding hodograph domain in PK), the free surface at point B_r is equivalent to B_2 of Figure 1(b). For finite but large k_1, there is still seepage through the whole segment B_rO (see Figure 4), and it is incorrect to assume the segment B_rM_1 in Figure 4 to be an impermeable boundary (as Wu et al. 2013 did). In their conceptual model, Wu et al. (2013) justified this artificial impermeable segment by the known phenomenon of capillary barrier. But even for a dam core with high capillarity, the flow topology near the interface in Figure 4 is different from what Wu et al. (2013) postulated.

In Figure 4, the streamline O_1OA does not experience any refraction. Therefore, there is a streamline between two bounding streamlines O_1OA and B_rM in Figure 4, which has the strongest refraction.

In Figure 4, there is no 'gap' of the seepage face like BB_2 in Figure 1(b). For $k_1 \gg k_0$ the segment B_rM of the free surface in the downstream shoulder is pretty close to B_rM_1. Near point B_r seepage in the shoulder resembles a thin vertical film. Consequently, what is above the dotted line MM_1 in Figure 4 can be approximated by a regular

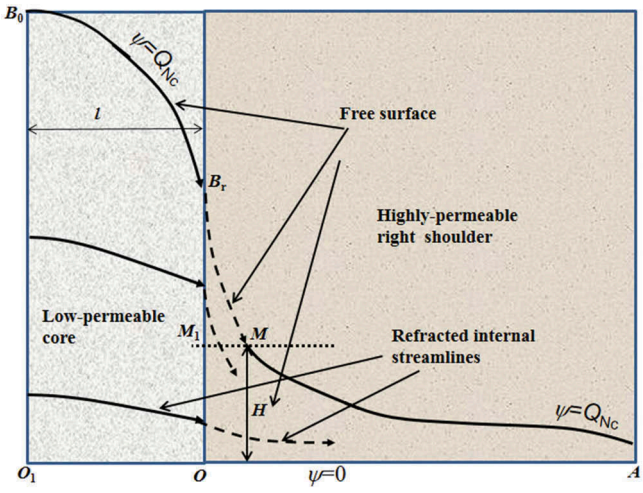

Figure 4. Refraction of the free surface and internal streamlines on the vertical interface between a low-permeable core and highly permeable downstream shoulder.

seepage face BB_2 (Figure 1(b)) in the PK solution to the dam problem.

The PK solution is mathematically complicated (see Kacimov and Obnosov 2016), except Charny's formula for the total flow rate:

$$Q_{Nc} = k_0 \frac{H_1{}^2 - H^2}{2l} \tag{11}$$

Equation (11) is exact and coincides with what the 1-D DF theory predicts (see PK for details).

Obviously, from conservation of mass $Q_N = Q_{Nc}$ and from Equations (11) and (7):

$$k_0 \frac{H_1{}^2 - H^2}{2l} = k_1 H \frac{I_0}{I_1} \tag{12}$$

Now dimensionless quantities $k^* = k_0/k_1$, $H_1^* = H_1/L_1$, $l^* = l/L_1$, $H^* = H/L_1$, $Q_{Nc}^* = Q_{Nc}/(k_1 L)$ are introduced. Then, Equation (12) can be re-written as:

$$k^*(H_1^{*2} - H^{*2})I_1 - 2H^* l^* I_0 = 0 \tag{13}$$

The quadratic Equation (13) is solved with respect to $H^*$for given values of k^*, H_1^*, l^*

and I_0/I_1 as a function of the affix a. The positive root of this equation is selected:

$$H^* = -l^* \frac{I_0}{k^* I_1} + \sqrt{H_1^{*2} + l^{*2} \frac{I_0{}^2}{k^{*2} I_1{}^2}} \tag{14}$$

Next, Equation (6) is engaged as:

$$H^* = \pi I_1 \left(\int_1^a \log \left[\frac{\varsigma + a^2 + \sqrt{a^2 - 1}\sqrt{a^2 - \varsigma^2}}{a(\varsigma + 1)} \right] \frac{\mathrm{d}\varsigma}{\sqrt{a^2 - \varsigma^2}\sqrt{\varsigma^2 - 1}} \right)^{-1} \tag{15}$$

Consequently, elimination of H^* from Equations (14) and (15) gives a single nonlinear equation with respect to a. This equation is solved by the **FindRoot** routine of *Mathematica*. After that H^* is found from either Equation (14) or (13) and $Q_{Nc}^* = Q_N^*$is evaluated from Equation (11). The results of computations of H^*as a function of k^* for l^* = 1/4,1/8 and 1/16 are shown in Figure 3(b), curves 1–3, correspondingly. These graphs display a significant increase of the locus of point B in Figure 1(b) with the increase of the core conductivity.

2.3. MODLFOW simulations

In this subsection, an FDM code, MODFLOW 2005, (Simcore, 2012) is used to solve the problem in Figure 1(b) taking into account both the upstream and downstream shoulders. In order to compare with Wu et al. (2013) specific dam dimensions were selected (Figure 5): the toe drain at the bottom of the upstream dam shoulder has a length of 5 m and is at zero head; the undrained upstream shoulder is also 5 m. All boundaries but the drain and reservoir in Figure 5 are impermeable. The dam core is of 0.5 m width, with various k_0 values. Both dam shoulders have k_1 = 2 m/day. The widths of the upstream shoulder are L_1 = 5 m. As the hydraulic resistance of the upstream shoulder is small, for simplification of the grid generation a rectangular upstream shoulder is selected as shown in Figure 5. The total width of the downstream shoulder is 10 m. A constant-head boundary of H_1 = 8 m is assigned to the vertical upstream shoulder.

The model area was gridded with 47 columns and 80 layers forming a total number of 3760 active cells. The spatial resolution of grid cells is more refined for the dam core and the area around it as illustrated by Figure 5 (Δx = 0.5 m to Δx = 0.1 m, whereas Δz = 0.1 m). The Preconditioned Conjugate Gradient (PCG2) solver has been selected for solving the steady flow equation with a convergence criterion of 0.001.

The results of computations are shown in Figure 6(a,b) for different core conductivity values. Figure 6(a) illustrates the free surface (water table) for three different k_0 values. As is evident from Figure 6(a), if the dam core becomes less permeable, the free-surface drops sharply across the core and the downstream shoulder. All seeping water is intercepted by the toe drain (computations do not show ponding above the toe). In the case of high k_0 = 0.1 m/day, the length (5 m) of the drain is too small to intercept all water seeped through the core and hence seepage occurs through the whole downstream shoulder. Figure 6(b) presents the velocity vectors and trajectories (streamlines) of marked particles released across the depth at the inlet vertical section of the upstream shoulder for k_0 = 0.01 m/day.

Oden and Kikuchi (1980, Figs 4.2–4.5), Lacy and Prevost (1987, Figure 7), Bardet and Tobita (2002, Fig.11), Herreros et al. (2006, Figs. 10,12), Darbandi et al. (2007, Fig.13), Bazyar and Graili (2012, Figs.15–16) studied similar rectangular two-zoned dams and found that the locus of a phreatic surface on a vertical interface between the zones is highly sensitive to the method used. Wu et al. (2013) numerically modeled saturated-unsaturated flow using the Richards equation. They also ignored the upstream, low hydraulic-resistance shoulder and considered a two-layered flow domain depicted in our Figure7. Wu et al. (2013) considered a tailwater filled up to 2 m of water depth. Below, a toe drain of a zero head is used, instead of a 2 m constant head in Wu et al. (2013). Instead of H_1 = 10 m in Wu et al. (2013), H_1 = 8 m is assumed such that the total head drop (8 m) across the dam is the same as in Wu et al.

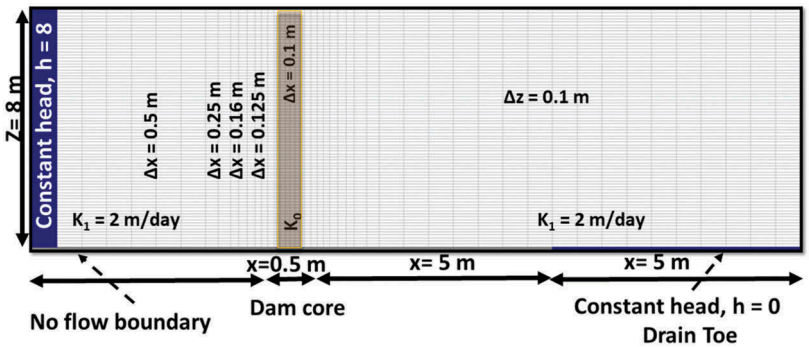

Figure 5. Vertical cross-section of the dam, MODFLOW 2005-simulated flow domain.

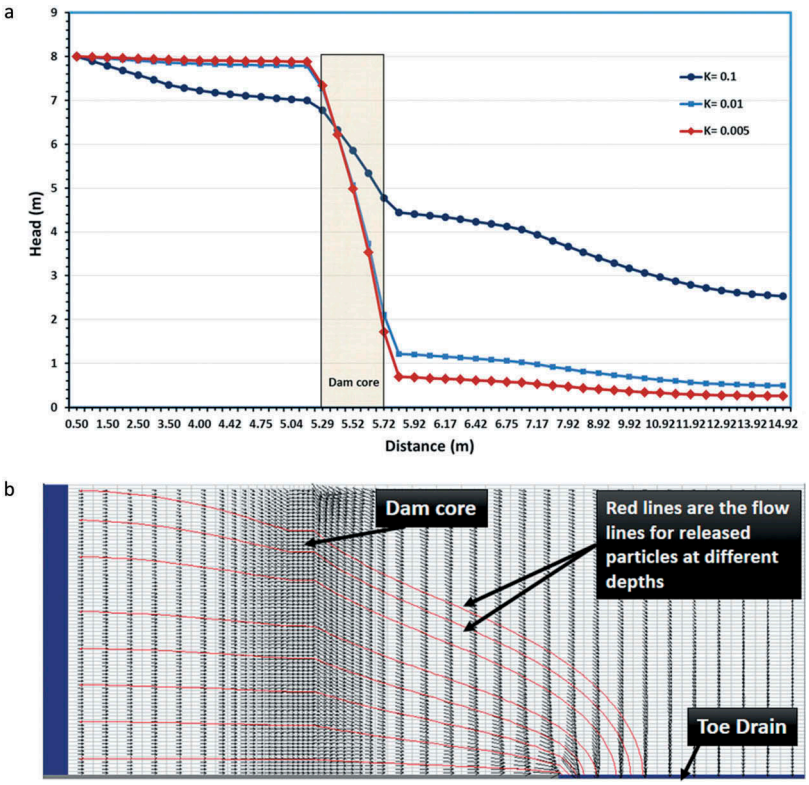

Figure 6. (a). Free surface (extracted from MODFLOW 2005 output files) in the two shoulders and the dam core for $k_0 = 0.1$, 0.01, and 0.005 m/day and $k_1 = 2$ m/day. (b). Trajectories of marked particles and velocity field for $k_0 = 0.01$ m/day in the middle vertical section of the MODFLOW 2005 model.

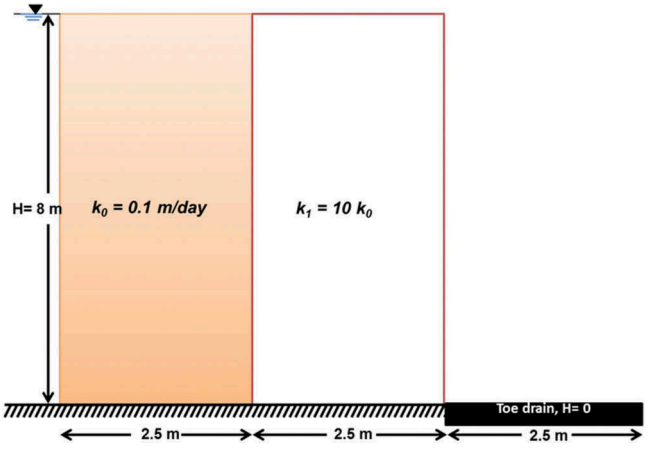

Figure 7. MODFLOW 2005-simulated flow domain of Wu et al. (2013) problem.

Dimensional values of k_0 (0.1 m/day) and k_1 (1 m/day) are kept the same as that used by Wu et al. (2013). Figure 8(a) presents the free surface in the two shoulders and core of the dam. This curve drops sharply in the core and has a mild slope in the shoulders. In Figure 8(b) we used the MODFLOW option of plotting streamlines by releasing marked particles at the inlet on the three-zone rectangular domain of Figure 7. Specifically, the red lines in Figure 8(b) depict the trajectories (pathlines) of these particles. The arrows illustrate the Darcian velocity vectors. Figure 8(b) illustrates that flow indeed converges towards the toe drain."

3. Concluding remarks

Safety of earth dams, especially aged ones, is a major concern of geotechnical engineers. They discover that seepage in zoned embankments, near drains, drain filters and at the downstream slope of the dams may cause collapse of the whole structure or its elements (see e.g. France et al. 2018). Therefore, a thorough analysis of seepage, in particular, the position of the phreatic surface and the quantity of water intercepted by the embankment toe drain (the main parameters of interest in this paper) have to be investigated for different dam-drain sizes and types of zonation. New analytical solutions and numerical simulations are needed for this analysis.

Casagrande (1937) pioneered in studies of phreatic flows in zoned porous dams. Aravin and Numerov (1953) also contributed to geotechnical and mathematical analysis of seepage through earth (rock) filled dams; they also pioneered in solving Hilbert's BVP for holomorphic functions. Inspired by Casagrande, Aravin and Numerov, in this paper we extended the Polubarinova-Kochina solution to the 'dam problem', *viz.* steady, essentially 2-D, free-surface flows through a low-permeable dam core conjugated with an adjacent highly permeable porous downstream shoulder towards an equipotential toe drain (horizontal filter).

In our analytical model, we ignored capillarity. Free-boundary problems for a harmonic function (total head and pressure head) are solved. Hydraulic coupling of the core and shoulder zones of the dam is carried out. Flow in the downstream shoulder of the dam is essentially 2-D. Near the core–shoulder interface, seepage is quasi-horizontal. Close to an unclogged toe drain (constant piezometric head segment) the phreatic surface (stream line) becomes vertical. The size of the 'active' segment of this drain is computed from the presented 2D analytical solution. The total seepage rate through the dam and the size of the 'active' segment of the drain

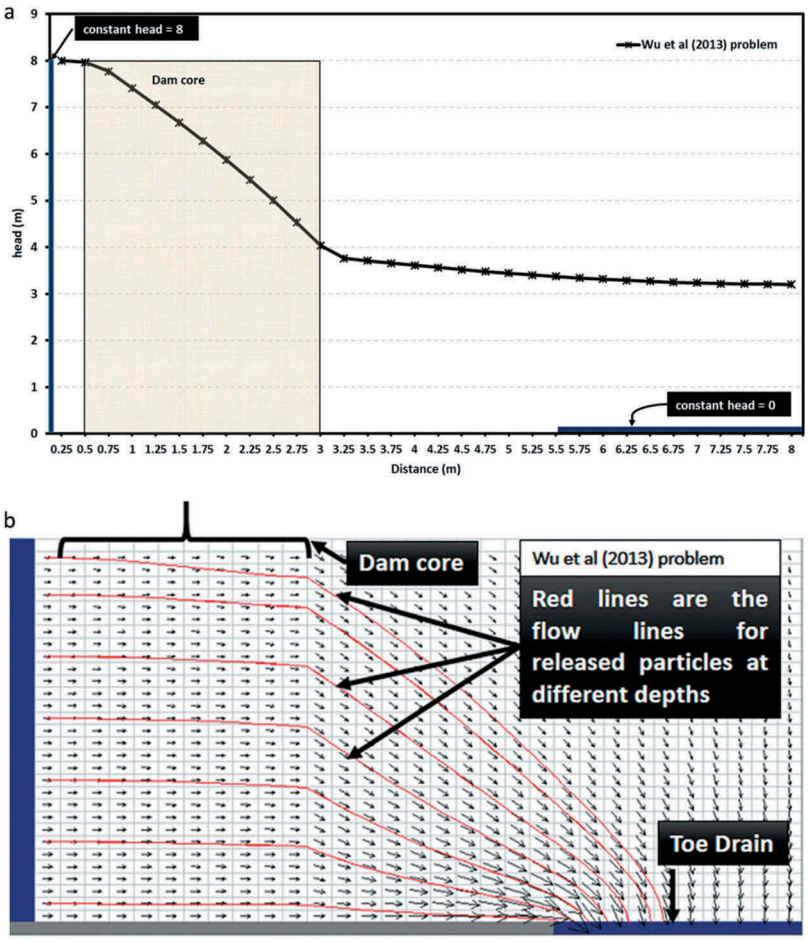

Figure 8. Free surface (extracted from MODFLOW 2005 output files) in the two shoulders and the dam core for k_0 = 0.1 m/day and k_1 = 1 m/day, see Wu et al. (2013) (a); Trajectories of marked particles and velocity field for the Wu et al. (2013) case (b).

are evaluated as functions of the sizes of the core and shoulder, distance to the tow drain and hydraulic conductivities of the two commingled subdomains. Simulations by MODFLOW 2005 allow to study seepage in piece-wise homogeneous porous dam bodies (there are no analytical solutions to this problem with refraction along with interfaces between the shoulders and core).

Acknowledgments

The research was funded by the subsidy allocated to Kazan Federal University for the state assignment in the sphere of scientific activities, project № 1.13556.2019/13.1. and by Sultan Qaboos University, Oman, grant IG/AGR/485 SWAE/14/02. Helpful comments by two anonymous referees are appreciated.

Disclosure statement

No potential conflict of interest was reported by the authors.

Funding

The research was funded by the subsidy allocated to Kazan Federal University for the state assignment in the sphere of scientific activities, project № 1.13556.2019/13.1. and by Sultan Qaboos University, Oman, grant IG/AGR/485 SWAE/14/02.

References

Al-Saqri, S., Al-Maktoumi, A., Al-Ismaily, S., Kacimov, A., and Al-Busaidi, H. (2016). "Hydropedology and soil evolution in explaining the hydrological properties of recharge dams in arid zone environments." *Arabian. J. Geosci.*, 9(1), 1–12. doi:10.1007/s12517-015-2076-0.

Aravin, V.I., and Numerov, S.N. (1953). *Theory of fluid flow in undeformable porous media*, Gostekhizdat, Moscow (in Russian). English Translation: Israel Program for Scientific Translation, Jerusalem, 1965.

Bardet, J.P., and Tobita, T. (2002). "A practical method for solving free-surface seepage problems." *Comput. Geotech.*, 29(6), 451–475. doi:10.1016/S0266-352X(02)00003-4.

Bazyar, M.H., and Graili, A. (2012). "A practical and efficient numerical scheme for the analysis of steady state unconfined seepage flows." *Int. J. Numer. Anal. Methods Geomech.*, 36(16), 1793–1812. doi:10.1002/nag.1075.

Borja, R.I., and Kishnani, S.S. (1991). "On the solution of elliptic free-boundary problems via Newton's method." *Comput. Methods Appl. Mech. Eng.*, 88(3), 341–361. doi:10.1016/0045-7825(91)90094-M.

Caffarelli, L.A., and Friedman, A. (1978). "The dam problem with two layers." *Arch. Ration. Mech. Anal.*, 68(2), 125–154. doi:10.1007/BF00281407.

Casagrande, A. (1937). "Seepage through dams." *J. N. Engl. Water Works*, 51, 295–336.

Cedergren, H.R. (1989). *Seepage, drainage and flow nets*, Wiley, New York, USA.

Chahar, B. (2004). "Determination of length of a horizontal drain in homogeneous earth dams." *J. Irrig. Drain. Eng., ASCE*, 130(6), 530–536. doi:10.1061/(ASCE)0733-9437(2004)130:6(530).

Crank, J. (1984). *Free and moving boundary problems*, Clarendon Press, Oxford.

Darbandi, M., Torabi, S.O., Saadat, M., Daghighi, Y., and Jarrahbashi, D. (2007). "A moving-mesh finite-volume method to solve free-surface seepage problem in arbitrary geometries." *Int. J. Numer. Anal. Methods Geomech.*, 31(14), 1609–1629. doi:10.1002/nag.611.

Design of small dams. (1987). USBR-ISDI, Washington. https://www.usbr.gov/tsc/techreferences/mands/mands-pdfs/SmallDams.pdf

FEMA (Federal Emergency Management Agency). (2011). *Filters for Embankment Dams – Best Practices for Design and Construction*. https://www.fema.gov/media-library/assets/documents/23795

France, J.W., Alvi, I.A., Dickson, P.A., FAlvey, H.T., Rigbey, S.J., and Trojanowksi, J., 2018. Independent Forensic Team Report: Oroville Dam Spillway Incident. https://damsafety.org/sites/default/files/files/IndependentForensicTeamReportFinal01-05-18.pdf

Friedman, A., Huang, S., and Yong, J. (1987). "Bang-bang optimal control for the dam problem." *Appl. Math. Optim.*, 15(1), 65–85. doi:10.1007/BF01442646.

Fukuchi, T. (2018). "New high-precision empirical methods for predicting the seepage discharges and free surface locations of earth dams validated by numerical analyses using the IFDM." *Soils Found.*, 58(2), 427–445. doi:10.1016/j.sandf.2018.02.011.

Gakhov, F.D. (1966). *Boundary value problems*, Pergamon Press, Oxford.

Gol'dshteˇın, R.V., and Entov, V.M. (1994). *Qualitative methods in continuum mechanics*, Longman, London.

Gradstein, I.S., and Ryzhik, I.M. (1962). *Tables of integrals, sums, series and products*, Nauka, Moscow.

Herreros, M.I., Mabssout, M., and Pastor, M. (2006). "Application of level-set approach to moving interfaces and free surface problems in flow through porous media." *Comput. Methods Appl. Mech. Eng.*, 195(1–3), 1–25. doi:10.1016/j.cma.2004.12.015.

ICOLD. (2013). *Internal erosion of existing dams, levees and dikes, and their foundations. bulletin. Volume 1: Internal erosion processes and engineering assessment*, ICOLD, Paris.

Ilyinsky, N.B., and Kacimov, A.R. (1992). "The estimation of integral seepage characteristics of hydraulic structures in terms of the theory of inverse boundary-value problems." *Zeitschrift Fur Angewandte Mathematik Und Mechanik*, 72(2), 103–112. doi:10.1002/zamm.19920720207.

Ilyinsky, N.B., Kacimov, A.R., and Yakimov, N.D. (1998). "Analytical solutions of seepage theory problems. Inverse methods, variational theorems, optimization and estimates (A review)." *Fluid Dyn.*, 33 (2), 157–168. doi:10.1007/BF02698697.

The international levee handbook. (2013). CIRIA, London. http://webissimo.developpement-durable.gouv.fr/IMG/pdf/A_The_International_Levee_Handbook_C731__cle7f8a33.pdf

Istomina, V.S. (1957). *Soil stability against seepage*, Gosstrojizdat, Moscow (in Russian).

Jaafar, H.H. (2014). "Feasibility of groundwater recharge dam projects in arid environments." *J. Hydrol.*, 512, 16–26. doi:10.1016/j.jhydrol.2014.02.054.

Junghanns, P., and Oestreich, D. (1989). "Numerische Lösung des Staudammproblems mit Drainage." *Zeitschrift Für Angewandte Mathematik Und Mechanik*, 69(2), 83–92. (in German). doi:10.1002/zamm.19890690213.

Kacimov, A.R., and Brown, G. (2015). "A transient phreatic surface mound, evidenced by a strip of vegetation on an earth dam." *Hydrol. Sci. J.*, 60(2), 361–378. doi:10.1080/02626667.2014.913793.

Kacimov, A.R., and Obnosov, Y.V. (2012). "Analytical solutions for seepage near material boundaries in dam cores: The Davison-Kalinin problems revisited." *Appl Math Model*, 36, 1286–1301. doi:10.1016/j.apm.2011.07.088.

Kacimov, A.R., and Obnosov, Y.V. (2016). "Size and shape of steady sea water intrusion, sharp-interface wedge: The Polubarinova-Kochina analytical solution to the dam problem revisited." *J. Hydrol. Eng., ASCE*, 21(8), 06016005-1-006016005-6. doi:10.1061/(ASCE)HE.1943-5584.0001385.

Kamble, R.K., Muralidhar, B., Hanumanthappa, M.S., Patil, A.V., and Edlabadkar, J.S. (2014). "Multiple approaches to analyse and control seepage in hydraulic structures." *ISH J. Hydraul. Eng.*, 20(1), 7–13. doi:10.1080/09715010.2013.821787.

Lacy, S.J., and Prevost, J.H. (1987). "Flow through porous media: A procedure for locating the free surface." *Int. J. Numer. Anal. Methods Geomech.*, 11(6), 585–601. doi:10.1002/nag.1610110605.

Liggett, J.A., and Liu, P.L.-F. (1979). "Unsteady interzonal free surface flow in porous media." *Water Resour. Res.*, 15(2), 240–246. doi:10.1029/WR015i002p00240.

Martin, S., and Vázquez, C. (2013). "Homogenization of the layer-structured dam problem with isotropic permeability." *Nonlinear Anal.*, 14(6), 2133–2151. doi:10.1016/j.nonrwa.2013.04.002.

Mishra, G.C., and Parida, B.P. (2006). "Earth dam with toe drain on an impervious base." *Int. J. Geomech., ASCE*, 6(6), 379–388. doi:10.1061/(ASCE)1532-3641(2006)6:6(379).

Mishra, G.C., and Singh, A.K. (2005). "Seepage through a levee." *Int. J. Geomech., ASCE*, 5(1), 74–79. doi:10.1061/(ASCE)1532-3641-(2005)5:1(74).

Moran, R., and Toledo, M.A. (2011). "Research into protection of rockfill dams from overtopping using rockfill downstream toes." *Can. J. Civ. Eng.*, 38, 1314–1326.

National Research Council. (2012). *Dam and levee safety and community resilience: A vision for future practice*, National Academies Press, Washington, DC.

Nichiporovich, A.A. (1973). *Dams of local materials*, Strojizdat, Moscow (in Russian).

Obnosov, Y.V., Kacimov, A.R., and Castro-Orgaz, O. (2015). "An exact analytical solution for steady phreatic flow disappearing/re-emerging towards/from a bedrock/caprock isobaric breach: The Polubarinova-Kochina-Numerov and Pavlovsky problems revisited." *Transp. Porous Media*, 108(2), 337–358. doi:10.1007/s11242-015-0522-9.

Oden, J.T., and Kikuchi, N. (1980). "Theory of variational inequalities with applications to problems of flow through porous media." *Int. J. Eng. Sci.*, 18(10), 1173–1284. doi:10.1016/0020-7225(80)90111-1.

Ouria, A., and Toufigh, M.M. (2009). "Application of Nelder-Mead simplex method for unconfined seepage problems." *Appl Math Model*, 33(9), 3589–3598. doi:10.1016/j.apm.2008.12.001.

Peter, P. (1982). *Canal and river levees*, Elsevier, Amsterdam.

Polubarinova-Kochina, P.Y. (1962). *Theory of ground water movement*, Princeton University Press, Princeton. Second edition of the book in Russian is published in 1977, Nauka, Moscow.

Rice, J.D., and Duncan, J.M. (2010). "Findings of case histories on the long-term performance of seepage barriers in dams." *J. Geotechnical Geoenviron.Eng., ASCE*, 136(1), 2–15. doi:10.1061/(ASCE)GT.1943-5606.0000175.

Simcore Software. (2012). *Processing modflow: An integrated modeling environment for the simulation of groundwater flow, transport and reactive processes*.

Strack, O.D.L. (2017). *Analytical groundwater mechanics*, Cambridge Univ. Press, Cambridge, UK.

Sumi, T. (2008). "Designing and operating of flood retention dry dams in Japan and USA." *Adv. Hydro-Sci. Eng.*, 8, 1768–1777.

Tanchev, L. (2014). *Dams and appurtenant hydraulic structures*, CRC Press, Boca Raton.

Tayfur, G., Swiatek, D., Wita, A., and Singh, V. (2005). "Case study: Finite element method and artificial neural network models for flow through Jeziorsko earthfill dam in Poland." *J. Hydraulic Eng. ASCE*, 131(6), 431–440. doi:10.1061/(ASCE)0733-9429(2005)131:6(431).

Wolff, T.F. (2002). Performance of levee under seepage controls: A critical review (Paper No. ERDC/GSL-TR-02-19). Vicksburg Lab.

Wolfram, S. (1991). *Mathematica. A system for doing mathematics by computer*, Addison-Wesley, Redwood City.

Wu, M.X., Yang, L.Z., and Yu, T. (2013). "Simulation procedure of unconfined seepage with an inner seepage face in a heterogeneous field." *Sci. China. Phys. Mech. Astron.*, 56(6), 1139–1147. doi:10.1007/s11433-013-5071-z.

Zhang, L.M., Peng, M., Chang, D., and Xu, Y. (2016). *Dam failure mechanisms and risk assessment*, Wiley, Singapore.

Zhilenkov, V.N. (1968). *Hydroisolation properties of soils making cores and liners in large dams*, Energiya, Leningrad (in Russian).